Comparative configurational study for He, Ne, and Ar trimers

T. González-Lezana
Instituto de Matemáticas y Física Fundamental, Consejo Superior de Investigaciones Científicas, Serrano, 123, 28006 Madrid, Spain

J. Rubayo-Soneira
Instituto Superior de Ciencia y Tecnología Nucleares, Ciudad de La Habana, 6163 Cuba

S. Miret-Artés
Instituto de Matemáticas y Física Fundamental, Consejo Superior de Investigaciones Científicas, Serrano, 123, 28006 Madrid, Spain

F. A. Gianturco
Department of Chemistry, The University of Rome, Cittá Universitaria, I-00185 Rome, Italy

G. Delgado-Barrio and P. Villarreal[a)]
Instituto de Matemáticas y Física Fundamental, Consejo Superior de Investigaciones Científicas, Serrano, 123, 28006 Madrid, Spain

(Received 26 October 1998; accepted 10 February 1999)

Helium trimer bound states are calculated by means of a variational method described in terms of atom pair coordinates and distributed Gaussian basis functions for zero total angular momentum. To show the feasibility of this method, we also apply it to the calculation of the first vibrational levels of the Ar_3 and Ne_3 clusters. Special emphasis is made on the study of the possible Efimov behavior of the first excited state found in the $^4He_3$ trimer. Geometrical configurations of the ground and first excited states of these rare gas trimers have been exhaustively studied owing to the proper symmetry of the coordinates chosen. © *1999 American Institute of Physics.* [S0021-9606(99)00218-4]

I. INTRODUCTION

Since the early studies in Nuclear Physics by Efimov on three-body (3B) systems built using nearly resonant two-body (2B) forces,[1] a lot of work has been carried out in order to analyze the physical implications of systems presenting this particularity, in case they do exist. The so-called Efimov effect appears whenever all the three pairs involved in a 3B system have no bound states but zero-energy resonances; then it is said that such a system supports infinitely many bound states which accumulate at the dissociation threshold. The same is true if any of the following criteria is satisfied:[2] (a) none of the pairs has bound states at all, (b) two of the pairs have zero-energy resonances, or (c) certain inequalities of the masses are satisfied. If the total 3B interaction potential is assumed to be the sum of the three 2B interactions affected by a strength parameter, λ, the number of bound states of the 3B system increases as this parameter is increased, eventually becoming infinite at a certain value of λ. However, some general comments should be made at this point. There is a rough evaluation of the number of such states for a 3B system, which depends on intrinsic properties of the 2B subsystems, given by[1,3]

$$N=\frac{1}{\pi}\ln\frac{|a|}{r_0}. \tag{1}$$

where a and r_0 are the scattering length and the effective range of the 2B potential, respectively. Only when the ratio between those two parameters is very large, would the system tend to show an infinite number of Efimov states. As far as we know, only some theoretical predictions on model 3B systems displaying this tendency have been reported.[4] The other point which one would need to further analyze is the disappearance of these 3B states when the λ parameter increases. Strengthening of the potential produces, in fact, a new (2B+1B) threshold which moves downward below the total fragmentation threshold. The Efimov states finally move to the continuum spectrum as they are overrun by the former threshold and become not real bound states any longer. They are usually called ghost states since they have no real existence.

In Molecular Physics, the most favorable candidates to present this effect are small He clusters; the dimer $^4He_2$, with the weakest bond ever observed, has a nearly zero-energy bound state and can lead to trimer formation where the Efimov states could in principle occur and be eventually observed.[5–8] $^4He_2$ was firstly detected by Luo *et al.*[9] collecting ion dimers after electron impact ionization. This finding was followed by some controversy about the likely sources of error in the interpretation of the possible neutral parents of the formed ions.[10–12] More recently, a nondestructive detection of ^4He_n with $n=2-10$ was conducted by Schöllkopf and Toennies[12] using diffraction techniques from a transmission grating.

A large number of theoretical studies has also been devoted to the study of He dimers and trimers.[5–7,13–19] Different results and conclusions concerning the total number of bound states and their main properties were found for the

[a)]Author to whom correspondence should be addressed.

trimer. Huber and Lim,[13] by using Faddeev equations, predicted one or two Efimov states depending on the 2B interaction potential employed. The Efimov behavior was found through the disappearance of these states as the strength of the potential was increased. In a further work, Huber[16] compared the number of Efimov states obtained in Ref. 13 with the estimate given by Eq. (1). Although this comparison was fairly good, the author recognized that his previous results were not conclusive. Lim *et al.*[5] found an Efimov state through similar calculations performed with one of the potentials used by Huber and Lim.[13] In fact, they reported two excited states above the ground level. The lowest of these excited states disappeared when the strength of the potential was increased only 1.01 times. Cornelius and Glöckle[6] used an old version of the Aziz *et al.* potential[20] within a Faddeev scheme as well. They concluded that the existence of one Efimov state could be surmised. Similar conclusions were achieved by Greene *et al.*[7] who, using an adiabatic approach in hyperspherical coordinates, established upper and lower limits to the energies of the ground and first excited states of $^4He_3$. In spite of all these results however, the presence of a single bound state has also been reported in the literature,[21,22] and even negative results about the existence of such Efimov states were found from scattering calculations.[14,23] Uang and Stwalley[14] obtained a value for N [from Eq. (1)] equal to 0.89, claiming the nonexistence of Efimov states. Huber[16] questioned such a conclusion and suggested to ''round up'' the results to the nearest appropriate integer. We could finally say that much of the controversy about the existence of Efimov states is mainly due to the uncertainties in our knowledge of the 2B interaction potential and only in part to the different theoretical methods applied to calculate the relevant bound states.

Properties of rare gas clusters have been the goal of several studies[21,22,24,25] (which in some cases did not include the ^{4}He trimer because of its extremely weak bond[21] and boson character). One of the conclusions usually drawn from such studies is the extreme floppiness of He clusters when compared with Ne and Ar clusters.[22] In the Monte Carlo (MC) calculations performed by Raman Krishna and Whaley,[19] average bond angles close to 60° were obtained, suggesting an equilateral triangle as the main geometrical configuration for the He trimer ground state. A similar result was reached by Rick *et al.*[22] and by Nielsen *et al.*[26] in their recent work. Nevertheless, recent MC studies have revealed a noticeable contribution coming from nearly linear geometries.[17] As will be shown below, our results agree with this last finding.

In this work, we present an alternative, more versatile, variational treatment to study boson triatomic systems. The procedure is developed using atom pair coordinates which provide a suitable way to tackle configurational studies. The same coordinates were already used to calculate variationally the rotation-vibration energies of H_3^+ and D_3^+.[27] Depending on the system under study, our procedure uses distributed Gaussian functions (DGF),[28] or standard orthonormal functions, to construct the corresponding symmetrized basis sets. These latter basis functions are inadequate to describe quasilinear configurations. On the contrary, the DGF set allows us a partial analytical representation of our Hamiltonian and facilitates the description of all types of contributing structures. For comparison, a detailed analysis for Ar, Ne, and He trimers is carried out by presenting bidimensional distribution functions and angular distributions. For Ar and Ne complexes, a comparative calculation using Jacobi coordinates has also been performed. On the other hand, the extremely diffuse nature of the He trimer precludes a similar calculation. We find in the latter case the existence of two 3B bound states; the excited level, while strictly speaking not a true Efimov state, we think presents several characteristics of the Efimov behavior which are extensively discussed in the present work. Moreover, special emphasis is addressed to the main geometrical configurations contributing to the He trimer bound states. From this kind of study, it is possible to envisage indirect ways to observe them.

II. METHOD

A. Hamiltonian

The Hamiltonian for zero total angular momentum, using atom–atom pair coordinates R_1, R_2, R_3, can be straightforwardly derived to be

$$H=\sum_{i=1}^{3}\left\{\frac{-\hbar^2}{m}\left[\frac{1}{R_i^2}\frac{\partial}{\partial R_i}R_i^2\frac{\partial}{\partial R_i}+\frac{R_j^2+R_k^2-R_i^2}{2R_jR_k}\frac{\partial^2}{\partial R_j\partial R_k}\right]+V(R_i)\right\};\quad i\neq j\neq k. \tag{2}$$

In these coordinates, the volume element is given by

$$d\tau=R_1R_2R_3dR_1dR_2dR_3. \tag{3}$$

Let Ψ be one of the eigenstates of the Hamiltonian (2). Then the transformation

$$\Phi=\sqrt{R_1R_2R_3}\Psi \tag{4}$$

leads to the standard normalization condition,

$$\int\int\int dR_1dR_2dR_3|\Phi|^2=1. \tag{5}$$

After the transformation given by Eq. (4), Φ becomes an eigenfunction of the effective Hamiltonian operator[8]

$$H=\sum_{i=1}^{3}\left\{\frac{-\hbar^2}{m}\left[\frac{\partial^2}{\partial R_i^2}+t_i\right]+V(R_i)\right\}, \tag{6}$$

where $V(R_i)$ is the 2B-interaction potential, with the t_i operators being

$$t_i=\frac{1}{R_i}\frac{\partial}{\partial R_i}-\frac{1}{4R_i^2}+\frac{R_j^2+R_k^2-R_i^2}{2R_jR_k}\left(\frac{\partial^2}{\partial R_j\partial R_k}-\frac{1}{2R_j}\frac{\partial}{\partial R_k}-\frac{1}{2R_k}\frac{\partial}{\partial R_j}+\frac{1}{4R_jR_k}\right) \tag{7}$$

with $i\neq j$, $j\neq k$, and $i\neq k$.

Notice that the Hamiltonian of Eq. (6) is totally symmetric under the change of any pair of particles and, by excluding the t_i operators, this Hamiltonian would strictly correspond to the sum of three 2B Hamiltonians.

TABLE I. Parameters for Morse potentials.

	D (cm^{-1})	α ($Å^{-1}$)	R_e (Å)
Ar–Ar	99.00	3.091	3.757
Ne–Ne	29.36	2.088	1.717

B. The potential energy surface (PES)

As usual, in this type of work, the PES for the system is described as the simple addition of realistic atom–atom interactions. For the ^{4}He trimer, the pairwise interaction was taken from Ref. 29. As regards the Ne and Ar trimers, simple Morse functions are used

$$V(R_i)=D[e^{-2\alpha(R_i-R_e)}-2e^{-\alpha(R_i-R_e)}]. \tag{8}$$

Values of the parameters for both clusters are shown in Table I. They come from numerical fittings, in the region of the well, of the potentials given by Aziz and Slaman for Ne–Ne (Ref. 30) and Ar–Ar (Ref. 31) and were previously obtained in Ref. 32.

The Lennard-Jones (LJ) potential is most commonly employed in the literature to describe the atom–atom interaction in Ne and Ar clusters.[21,22,24,25] For Ar_3, an alternative potential suggested by Aziz and Slaman[31] has also been used.[24] Nevertheless, our study on Ne and Ar clusters does not intend to achieve results which crucially depend on using a highly accurate interaction potential since our goal is to compare the main features of the lowest levels of these clusters with those obtained for $^4He_3$. Due to the likely existence of only two bound states for that cluster, a fairly precise description of the first levels is all we require. Moreover, a comparison between results obtained using a LJ potential[25] and the potential suggested by Aziz previously noted[31] did not reveal a particularly good agreement.[24]

Absence of many-body contributions to the potential for He clusters, as it was previously pointed out,[7] is justified by *ab initio* and MC calculations carried out by Parish and Dykestra and Bhattacharya and Anderson,[33] respectively. Similar calculations were conducted to study the role of the 3B forces in Ar_3.[24] The final conclusion was that long-range 3B interactions affect the vibrational spectrum of this cluster and inclusion of Axilrod–Teller and double-dipole-quadrupole terms should be considered. As very high accuracy for the calculations involving Ne and Ar clusters is not our main aim at the moment, those terms were not included in the present calculations.

Finally, for a comparison of a number of modern helium–helium potentials, see Ref. 34.

C. Basis functions

In most of the previous works, orthonormal basis sets were considered. However, it is difficult to describe linear configurations using such basis sets, and since the He trimer seems to also explore this type of arrangements, we have to resort to nonorthogonal basis functions to account for such situations. The eigenfunctions of the total Hamiltonian are expanded in terms of basis functions as

$$\Phi_k(R_1,R_2,R_3)=\sum_j a_j^{(k)}\phi_j(R_1,R_2,R_3), \tag{9}$$

where k stands for the ordering number of the bound states and j denotes a collective index, $j=(l\leqslant m\leqslant n)$. The ϕ_j functions are built up as symmetrized products of pair functions as follows:

$$\phi_j(R_1,R_2,R_3)=N_{lmn}^{-1/2}\sum_{P\in S_3} P[\varphi_l(R_1)\varphi_m(R_2)\varphi_n(R_3)], \tag{10}$$

where the coefficients

$$N_{lmn}=6(s_{ll}s_{mm}s_{nn}+s_{ll}s_{mn}^2+s_{mm}s_{ln}^2+s_{nn}s_{lm}^2+2s_{lm}s_{ln}s_{mn}) \tag{11}$$

define normalization factors expressed in terms of overlaps written as

$$s_{pq}=\langle\varphi_p|\varphi_q\rangle. \tag{12}$$

Basically, each $\phi_j(R_1,R_2,R_3)$ function describes a triangular configuration in such a way that it represents the six possible triangular arrangements formed when the R_1, R_2, and R_3 sides are equal to the centers of the Gaussian functions R_l, R_m, R_n, respectively. Although the basis set given by Eq. (10) is not orthogonal, the pseudoeigenvalue problem originated by this procedure can be transformed to a standard eigenvalue problem by using the method developed by Löwdin.[35]

As suggested by Hamilton and Light,[28] the one-dimensional function φ_p is chosen to be a DGF centered at the R_p position

$$\varphi_p(R_i)=\sqrt[4]{\frac{2A_p}{\pi}}e^{-A_p(R_i-R_p)^2}. \tag{13}$$

The coefficients A_p are defined in terms of the distance between centers of consecutive Gaussian functions as follows

$$A_p=\frac{4\beta}{(R_{p+1}-R_{p-1})^2}, \tag{14}$$

where β is a dimensionless parameter close to one. In order to fulfill the triangular requirement

$$|R_1-R_2|\leqslant R_3\leqslant R_1+R_2, \tag{15}$$

the product $\varphi_l\varphi_m\varphi_n$ will belong to the basis if the corresponding DGF centers verify that

$$R_n\leqslant R_l+R_m. \tag{16}$$

The scheme of construction of the $\phi_j(R_1,R_2,R_3)$ basis functions is based on the following steps. First, three Gaussian functions satisfying the triangle requirement (16) are chosen, one for each center placed in the R_i coordinate; thus, the first values of each R grid are taken for R_1, R_2, and R_3 in the ϕ_1 function. Second, ϕ_2 is built with R_1,R_2 fixed and the next value of the grid for R_3; this is successively repeated until a nonacceptable value [in the sense of Eq. (16)] for R_3 is reached. Third, R_2 changes its value from the old one to the next point in the grid, while R_3 is running through all the values of the grid until it reaches again another nonacceptable value. Finally, the same procedure is followed for the remaining points of the R_1 grid.

This procedure should provide exact results in the limit of infinite δ functions as starting basis functions.[28] In practice, however, one has to deal with a finite number of Gaussian functions of nonzero width. So some tests to guarantee the quality of the variational calculation need to be verified. Due to the fact that the total wave function is finally obtained, three tests based on the evaluation of statistical quantities have been carried out:

(1) The values of $\langle \cos\theta \rangle_k$ and $\langle \cos^2\theta \rangle_k$ has to be within the limits $[\frac{1}{3}, \frac{1}{2}]$, $[\frac{1}{4}, 1]$, respectively. The θ angle is here any of the three angles of a triangle.

(2) The values of $\langle S \rangle_k$ and $\langle S^2 \rangle_k$, S being the area of the triangle, should be always positive and fulfill the condition $\langle S^2 \rangle_k \geqslant \langle S \rangle_k^2$.

(3) The deviations from the triangle requirement (DTR) defined as

$$\mathrm{DTR}^{(k)} = 1 - \int_0^\infty dR_1 \int_0^\infty dR_2 \int_{|R_1-R_2|}^{R_1+R_2} |\Phi_k(R_1,R_2,R_3)|^2 dR_3 \tag{17}$$

should be very small. While the first two tests provide the necessary constraints to reject the ill-behaving basis sets, the last one allows us to decide among the different acceptable basis sets that minimize DTR.

Once the basis set is finally selected, several distribution functions can be evaluated in order to have some geometrical indicators about the bound states. Thus, the pair distribution $D^{(k)}(R_1)$ function, for each k-bound state, is defined as

$$D^{(k)}(R_1) = \int \int |\Phi_k(R_1,R_2,R_3)|^2 dR_2 dR_3, \tag{18}$$

and, analogously, the bidimensional probability density function, $\mathcal{D}^{(k)}(R_1,R_2)$, as

$$\mathcal{D}^{(k)}(R_1,R_2) = \int |\Phi_k(R_1,R_2,R_3)|^2 dR_3. \tag{19}$$

D. Statistical quantities and angular distributions

An additional advantage of using such pair coordinates resides in the fact that averages and fluctuations (and higher momenta) of any quantity associated with a triangle configuration are easily obtained. As has been said before, each ϕ_j basis function is related to a triangular configuration and, therefore, quantities such as the area (from the Heron formula), cosine values of any angle of a triangle (from the cosine theorem) or the diameter of the circumscribed circumference (from the sine theorem) can be evaluated in order to extract the angular distributions and most probable geometries of the corresponding bound states of the trimer system under study. However, starting with the values for each side of a triangle, the evaluation of the area involves a square root and therefore its average value over all possible configurations, calculated from the total wave function, can not be easily carried out. In general, the evaluation of any other statistical quantity with the same procedure is very time consuming and cumbersome due to the large number of configurations contributing to the bound states for very floppy systems. An alternative and easier way to proceed has been developed leading to similar results.

From the normalization condition of the total wave function and its definition in Eq. (9), a sort of weight, $P_j^{(k)}$, can be extracted for each j configuration as follows:

$$1 = \langle \Phi_k | \Phi_k \rangle = \sum_j a_j^{(k)} \langle \Phi_k | \phi_j \rangle = \sum_j P_j^{(k)}, \tag{20}$$

where, although the sum of the quantities $P_j^{(k)}$ is effectively equal to one, their values (not always positive) prevent them from being considered as proper statistical weights. Despite this drawback, they enable us to estimate the number and type (linear, isosceles, equilateral, and scalene) of triangle configurations present in the triatomic system. In order to classify them, a certain minimum variation on the sides of the triangles has to be accepted. Obviously, the minimum step size of the R_i grid is the natural choice for such dispersion.

Thus with these pseudoweights, the momenta of a given magnitude x for the k bound state can be calculated as (resorting to the mean value theorem)

$$\langle x^n \rangle_k = \sum_j a_j^{(k)} \langle \Phi_k | x^n | \phi_j \rangle \approx \sum_j P_j^{(k)} x_j^n, \tag{21}$$

where in the integrals involved we have assumed that the magnitude x depending on the three pair coordinates has been replaced by a mean value corresponding to the triangle configuration described by the ϕ_j function. In particular, some derivative magnitudes such as the root mean square $\sqrt{\langle x^2 \rangle}$ and the mean-square deviation or dispersion $\sigma^2 = \langle x^2 \rangle - \langle x \rangle^2$ can be easily extracted.

III. RESULTS

We start this section by showing the results (some levels of the vibrational spectrum and geometrical configurations) for the Ar_3 and Ne_3 trimers in order to illustrate the applicability of the method proposed in this work. The success of this test will permit us to extend the same procedure to boson triatomic systems like the He_3 trimer. A different treatment for the He clusters when comparing with other rare gas systems has been discussed.[21,22] Leitner *et al.*[21] could not study $^4He_3$ using the equally spaced discrete variable representation (DVR) as they did with Ne, Ar, Kr, and Xe, and Rick *et al.*[22] had to use different trial functions in their MC calculations in order to study He, Ne, and Ar clusters, because of the differences found in the rigidity of their corresponding ground states.

A. Numerical details

The calculations for He_3 clusters have been performed employing 39 Gaussian functions, 17 of them equally spaced with intervals of 0.5 Å in the region of the 2B potential well (3–11 Å) and the rest covering up to 139 Å with increasingly larger spacing; in all we used 2944 total symmetrized ϕ_j functions. However, some of the details need to be further explained. The numerical convergence is quite critical for this system and the statistical magnitudes mentioned above have been used as criteria to choose a good basis set. Thus, for example, if one additional Gaussian function is included at 11.5 Å, although the ground level is found to be reason-

TABLE II. First energy levels for Ar_3 expressed with respect to the bottom of the potential well (297 cm^{-1}). First column is taken from Ref. 24 with the assigned hyperspherical vibrational modes in parenthesis, second column is obtained from Jacobi coordinates, and third and fourth columns come from using pair coordinates with orthogonal basis functions (OBF) and DGF (see text), respectively. In the last two columns, only totally symmetric levels are listed. The ± signs stand for a basis including even or odd diatomic rotational quantum numbers, respectively.

	Ref. 24	Jacobi	OBF	DGF
(000)	43.72	44.55 (+)	44.56	44.57
(001)	66.49	67.62 (−)		
(010)	66.76	67.88 (+)		
(100)	76.64	75.95 (+)	76.08	76.09
(002)	82.21	82.02 (+)		
(020)	87.76	88.80 (+)	88.81	88.83
(011)	88.90	89.20 (−)		
		90.23 (+)		
(110)	97.61	95.59 (−)		
(101)	97.66	96.41 (+)		
(200)	106.49	103.59 (+)	103.50	103.55
(003)	106.56	106.51 (−)		
(030)	107.33	107.76 (+)	108.11	108.20
(012)	108.56	111.59 (−)		
(021)	109.19	112.17 (+)		
(120)	116.71	114.73 (−)		
(111)	117.18	115.11 (+)		
(102)	117.90	117.89 (+)	116.19	116.88
		119.52 (−)		

ably described, the average value of the area associated can be negative and, therefore, this particular point can not be included in our basis set. An additional parameter to adjust is β which controls the width of the Gaussian function given by Eq. (14). Obviously, different values of this parameter can make acceptable that point discarded before. By using $\beta = 1.10$ with the present extended basis, similar statistical magnitudes for the ground level are reproduced, although a slightly unbound first excited state is obtained. Finally, a value of $\beta = 1.05$ for the original points mentioned above yielded an acceptable basis set for which the DTR values defined by Eq. (17) are lower than 2%.

For Ne_3, 15 Gaussian functions have been taken, from 2.6 to 5.4 Å, equally spaced with intervals of 0.2 Å, which generated 678 symmetrized ϕ_j functions. Similarly, 11 Gaussian functions, centered from 3.0 to 5.0 Å with the same interval as Ne_3 have been used for Ar_3 with a total number of 286 symmetrized ϕ_j functions. Thus the numerical convergence for both trimers with all of the requirements above mentioned is easily achieved.

B. Ar_3 and Ne_3 clusters

In Table II, a comparison of the first energy levels for Ar_3 measured from the bottom of the potential well ($3 \times 99.0\ cm^{-1}$) is presented when different coordinates and basis sets are used. In the first column, the levels reported in Ref. 24, obtained through a self-consistent-field-configuration-interaction (SCF-CI) treatment in hyperspherical coordinates, are listed and assigned to different vibrational modes. The second column corresponds to our variational levels obtained using Jacobi coordinates. The ± signs stand for a basis including either even or odd diatomic rotational states, respectively. Finally, in the third and fourth columns, our results in terms of pair coordinates are presented when orthogonal basis functions (OBF) and DGF are employed, respectively. In these three last columns, the levels are listed following a criterion of proximity in energy with respect to the values of the first column. The calculations of Ref. 24 were performed using the Aziz's potential[31] and also included 3B interactions. As one can be see, the agreement is fairly good for the first levels of the vibrational spectrum. Due to the proper construction of the basis functions, our results in the third and fourth columns only correspond to totally symmetric vibrational motions. Notice also that the levels of energies 90.23 and 119.52 cm^{-1} coming from the variational Jacobi calculation were not reported by the SCF-CI treatment.

Other methods applied to this system are those based on MC calculations [diffuse (DMC) and variational (VMC) MC methods[22]] and on the successive diagonalization-truncation (SDT) method[21] within a DVR scheme. As is well known, MC calculations only provide the first vibrational state. The DMC result was 36.94 cm^{-1} and the VMC result 38.40 cm^{-1} which are less deep than our results for the ground state. The result for the DVR calculations[22] was a first level of 37.09 cm^{-1}. The LJ potential well depth used in both calculations was 82.99 cm^{-1}.

For a further comparison, energies for the ground ($k = 0$) and first ($k = 1$) excited vibrational states as well as average triangle sides, areas, and cos θ are reported in Table III for the three trimers: Ar_3, Ne_3, and He_3. In parenthesis, the corresponding root mean square is also included. The value obtained for $\langle R \rangle_0$, being R any side of the triangle in the ground state of the trimer Ar_3, compares well with 3.91 ± 0.20 Å given by Rick *et al.*[22] and the area of the equilateral triangle calculated with this side, 6.35 $Å^2$, is really close to our result for $\langle S \rangle_0$. The same calculation furnishes a value of 6.59 $Å^2$ for the first excited state, only slightly higher than

TABLE III. Results for the ground ($k = 0$) and first ($k = 1$) excited vibrational states of the Ar_3, Ne_3, and He_3 systems: energy, average triangle side, area, and cos θ. In parenthesis, the root mean square of the last three magnitudes.

	Ar_3		Ne_3		He_3	
	$k=0$	$k=1$	$k=0$	$k=1$	$k=0$	$k=1$
E (cm^{-1})	−252.43	−220.91	−50.23	−33.81	−0.1523	−0.0012
$\langle R \rangle$ (Å)	3.83(3.83)	3.90(3.91)	3.31(3.32)	3.61(3.66)	7.88(8.71)	50.03(57.28)
$\langle S \rangle$ ($Å^2$)	6.33(6.34)	6.56(6.59)	4.68(4.71)	5.26(5.32)	15.03(26.23)	684.31(994.01)
$\langle \cos \theta \rangle$	0.499(0.502)	0.498(0.503)	0.496(0.507)	0.480(0.553)	0.396(0.818)	0.402(0.739)

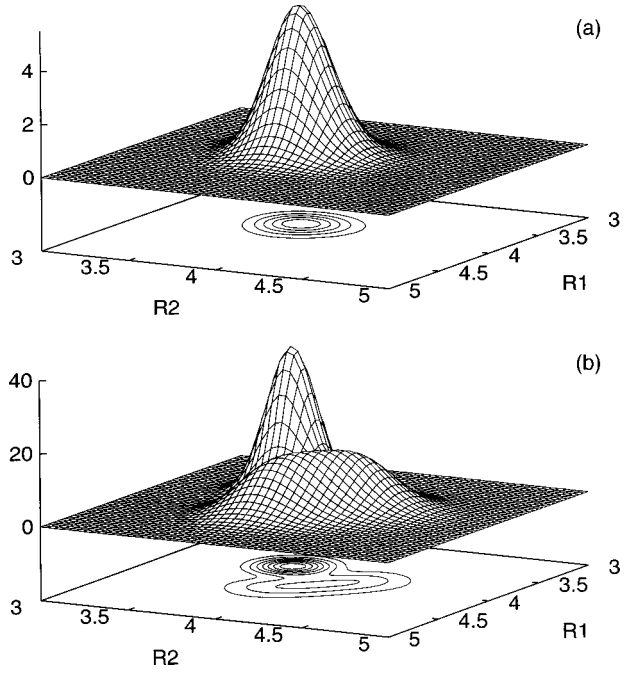

FIG. 1. Ar_3 three-dimensional plots, $\mathcal{D}^{(k)}(R_1,R_2)$, for (a) the ground ($k=0$), and (b) first excited ($k=1$) states. Units for R_1 and R_2 are in Å. For the first excited state, the function has been multiplied by 10.

ours. Average values of cos θ for both states also suggest the predominance of the equilateral arrangement.

In Figs. 1(a) and 1(b), the three-dimensional and contour plots of the $\mathcal{D}^{(k)}(R_1,R_2)$ functions for the ground ($k=0$) and first ($k=1$) excited states are shown, respectively. $\mathcal{D}^{(0)}(R_1,R_2)$ is clearly centered at $R_1=R_2=3.80$ Å, whereas $\mathcal{D}^{(1)}(R_1,R_2)$ has a maximum peak at 3.73 Å with a suggested shoulder around 4.10 Å. The pair distribution function showed by Horn *et al.*[24] for the ground level was sharply peaked at 3.76 Å, indicating the good agreement with our result. Notice that both densities are very much compressed in a small region of the (R_1,R_2) space.

Finally, also for comparison, the pseudoweights $P_j^{(k)}$ of the different triangular configurations are presented in Table IV for the three trimers. In the first column, the results correspond to the Ar_3 cluster. According to this table, a clear dominance of the equilateral structure, 71.1%, for the ground state, is found again. For the first excited state, we have: 52.5% for the equilateral structures and only 32.9% for the isosceles configurations. Rick *et al.*[22] also reported an average bond angle equal to 60° for the ground level. Predominance of equilateral configurations was also suggested by

TABLE IV. Percentages (pseudoweights) on the different types of triangular arrangements, $P_j^{(k)}$.

	Ar_3		Ne_3		He_3	
	$k=0$	$k=1$	$k=0$	$k=1$	$k=0$	$k=1$
Quasilinear	0.0	0.0	0.0	0.0	27.1	3.7
Scalene	16.2	14.6	23.4	38.8	48.3	74.3
Isosceles	12.7	32.9	45.0	51.7	23.6	21.7
Equilateral	71.1	52.5	31.6	9.5	1.0	0.3

TABLE V. First Ne_3 vibrational bound states (in cm^{-1}). In the first column, results from DVR and hyperspherical coordinates calculations by Leitner *et al.* (see Ref. 21) are listed, the second and third columns come from diffusion (DMC) and variational (VMC) Monte Carlo calculations by Rick *et al.* (see Ref. 22), respectively. Last two columns correspond to our calculations with Jacobi coordinates and the DGF basis set.

k	Ref. 21	DMC (Ref. 22)	VMC (Ref. 22)	E_k^{Jacobi}	E_k^{DGF}
0	−42.51	−42.58	−42.18	−49.88	−50.23
1	−30.19			−33.75	−33.81
2	−28.16			−29.56	−27.53

Horn *et al.*[24] as they found a similarity of the hyperspherical modes used in their study with the degenerate normal modes of an equilateral X_3 system.

Results for the first vibrational levels of the spectrum of the Ne trimer are presented in Table V with different coordinates and methods. Our DGF energies (last column) correspond to totally symmetric states deeper than those from the previously mentioned MC[22] and SDT[21] calculations. This finding is due to the smaller Ne–Ne potential depth, 24.74 cm^{-1}, employed in that work. The comparison between results from internal and Jacobi coordinates calculations is fairly good. In Table III, triangular statistical magnitudes for the two first energy levels, $k=0$ and $k=1$, are listed in the third and fourth columns. In Figs. 2(a) and 2(b), the $\mathcal{D}^{(k)}(R_1,R_2)$ functions are also displayed for the ground ($k=0$) and first ($k=1$) excited states, respectively. The probability density for the ground level, $\mathcal{D}^{(0)}(R_1,R_2)$, is clearly centered at $R_1=R_2=3.23$ Å with $\langle R\rangle_0=3.31$ Å (which compares quite well with the result obtained by Rick *et al.*, 3.37 ± 0.34 Å), whereas the first excited level shows a bimodal behavior with maxima at 3.20 and 4.24 Å, respectively,

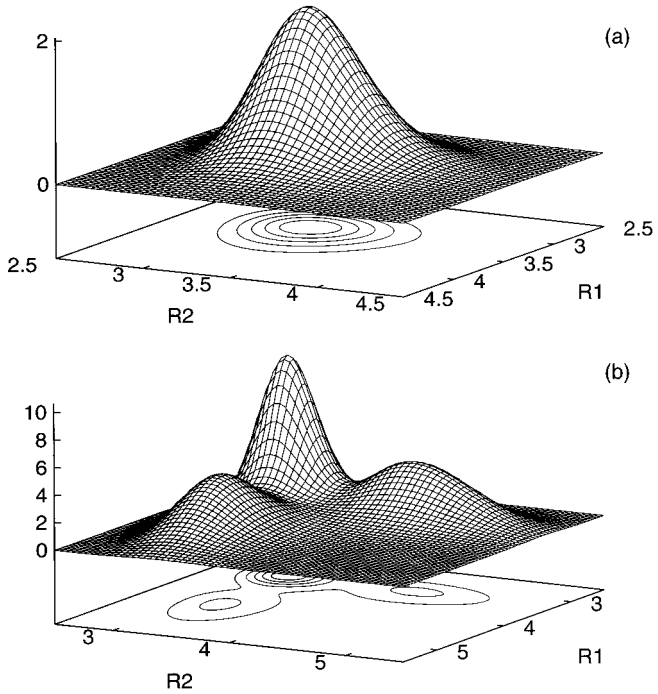

FIG. 2. Same as in Fig. 1 for Ne_3. The $\mathcal{D}^{(1)}(R_1,R_2)$ function has been multiplied by 10.

with $\langle R\rangle_1 = 3.61$ Å. As expected, both bound levels present a less compressed spatial distribution with respect to the line $R_1 = R_2$ suggesting a less rigid geometry compared with that for Ar_3 case.

From Table IV, the analysis of the different triangular arrangements for $k=0$ reveals a clear dominance of isosceles configurations and a decreasing contributions from equilateral structures. Nevertheless, the area of an equilateral triangle with sides equal to the value obtained for $\langle R\rangle_0$ is 4.68 Å^2, close to the value shown in Table III. Moreover, the value obtained for $\langle \cos\theta\rangle_0$ stresses the equilateral contribution. It should be also noted that an equilateral configuration has been previously predicted for the Ne_3 ground state.[21,22] Rick *et al.*[22] again obtained an average bond angle of 60 degrees and found the peak of the wave function localized at this triangular configuration. Similar conclusions were reported by Leitner *et al.*[21] The first excited state presents a considerably lower contribution from such structures although the area calculated from the side $\langle R\rangle_1 = 3.61$ Å and the value of $\langle \cos\theta\rangle_1$ nearly equal to 0.5 would indicate a geometry not very far from the equilateral one. This apparent contradiction is attributed to the fact that most of the isosceles structures are very nearly equilateral.

C. He_3 clusters

The He_3 cluster has already been subject of several studies in order to detect possible Efimov states.[5–8,13,15,16,23] According to Eq. (1), the predicted number of Efimov states for this system is ≈0.8, with $a = 100.13$ Å and $r_0 = 7.35$ Å issued from to the potential used in this work. Our previous analysis of this problem[8] concluded the existence of two bound states with energies -0.15 cm^{-1} for the ground state and -1.24×10^{-3} cm^{-1} for the excited level. Values of the main characteristic features are shown in the last two columns of Table III. From this table, the $\langle R\rangle_0$ value for the ground state is slightly smaller than the results previously reported: 9.22 ± 4.73 (Ref. 22) and 9.9 ± 5.3 Å.[19]

In Figs. 3(a) and 3(b), three dimensional probability distributions for both states, $k=0$ and $k=1$, respectively, confirm the great difference between the spatial extension of the two states. Compared with the two other trimers, the He trimer clearly reveals a more dispersed nature with higher values of the standard deviations for almost all the magnitudes calculated. Spatial extension is considerably large for the $k=1$ state as may be expected from the weakly bound 2B system (-0.91×10^{-3} cm^{-1}). The striking feature is found to be the average distance for the excited state, 50.03 Å, while the mean root square is 57.28 Å. As it was previously noted,[1,8] this is one of the main aspects of systems with an Efimov behavior. The $\mathcal{D}^{(0)}(R_1,R_2)$ distribution function for the ground state [in Fig. 3(a)] shows a bimodal structure with maxima located at 4.53 and 8.81 Å. This bimodal distribution can be interpreted as being due to the presence of quasilinear geometrical configurations as will be discussed below. Both distributions are spatially orthogonal in the sense that $\mathcal{D}^{(1)}(R_1,R_2)$ has negligible values in the region where $\mathcal{D}^{(0)}(R_1,R_2)$ is defined. This extremely diffuse and delocalized nature of the He trimer was also reported in some MC calculations (see Table V).[19,22]

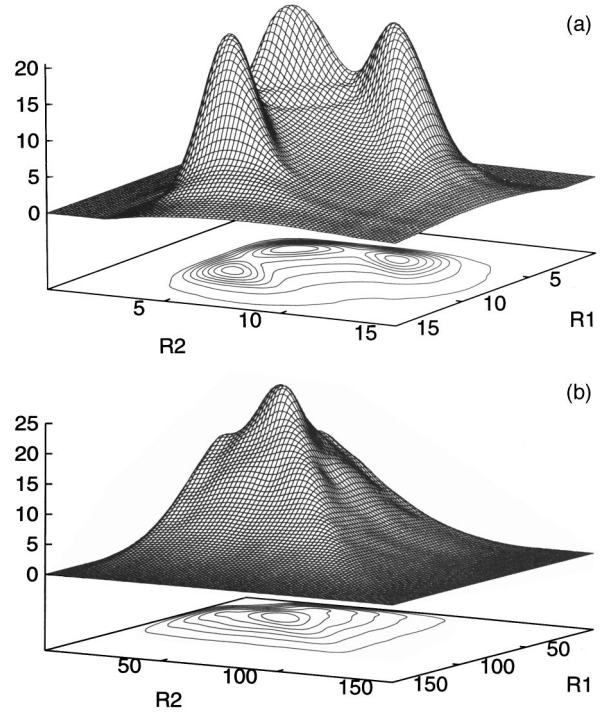

FIG. 3. Same as Fig. 1 for He_3. The $\mathcal{D}^{(0)}(R_1,R_2)$ function has been multiplied by 10^3 and $\mathcal{D}^{(1)}(R_1,R_2)$ by 10^5.

In Table VI, the 3B energies are compared with previous works. Although the energy of the trimer ground state is one of the deepest, it is clearly between the limits reported by Greene *et al.*[7] in his adiabatic hyperspherical study. The value for the excited state is similar to the energy found in the most recent works.[6,7,15,23]

TABLE VI. Different He trimer and dimer levels reported in the literature are listed. E_0^{3B} and E_1^{3B} correspond to energies of the ground and first excited levels of the trimer, respectively, whereas E_0^{2B} is the energy of the ground level for the dimer. Results in the fourth column are expressed in powers of 10 in parenthesis. As explained in the text, (*) means that another excited state was found although nothing is said about its possible Efimov behavior, and (**) means that two Efimov states are found for the potential used. Small letters in parenthesis refer to the potential used in each calculation: [a]See Ref. 36, [b]see Ref. 37, [c]see Ref. 38, [d]1.00098 times the potential from Ref. 39, [e]1.001 times the potential from Ref. 40, [f]Aziz's 1979-version from Ref. 20, [g]Aziz's 1987 version from Ref. 41, [h]latest Aziz's version from Ref. 29 and [i]from Ref. 42. Values in parenthesis from Greene's results are lower limits to the energies of the trimer.

Ref.	E_0^{3B} (cm^{-1})	E_1^{3B} (cm^{-1})	E_0^{2B} (cm^{-1})
5	−0.0598	−0.0066*	[a]
13	−0.1043	−0.0047	−3.8 (−3)[b]
	−0.0605	−0.0008	−0.3 (−3)[a]
	−0.0487	−0.0002**	−7.3 (−6)[c]
	−0.0459	−0.0002**	−3.7 (−6)[d]
	−0.0466	−0.0001**	−9.0 (−8)[e]
23	−0.0639	−0.0007	−0.58 (−3)[f]
6	−0.0764	−0.0011	−0.58 (−3)[f]
19	−0.0799		[g]
7	−0.0737 (−0.2041)	−0.0015 (−0.0024)	−0.91 (−3)[h]
	−0.0692 (−0.1925)	−0.0011 (−0.0019)	−0.58 (−3)[f]
17	−0.0829		−0.76 (−3)[i]
15	−0.0584	−0.0010	−0.58 (−3)[f]
	−0.0667	−0.0017	−1.17 (−3)[g]
8	−0.1523	−0.0012	−0.91 (−3)[h]

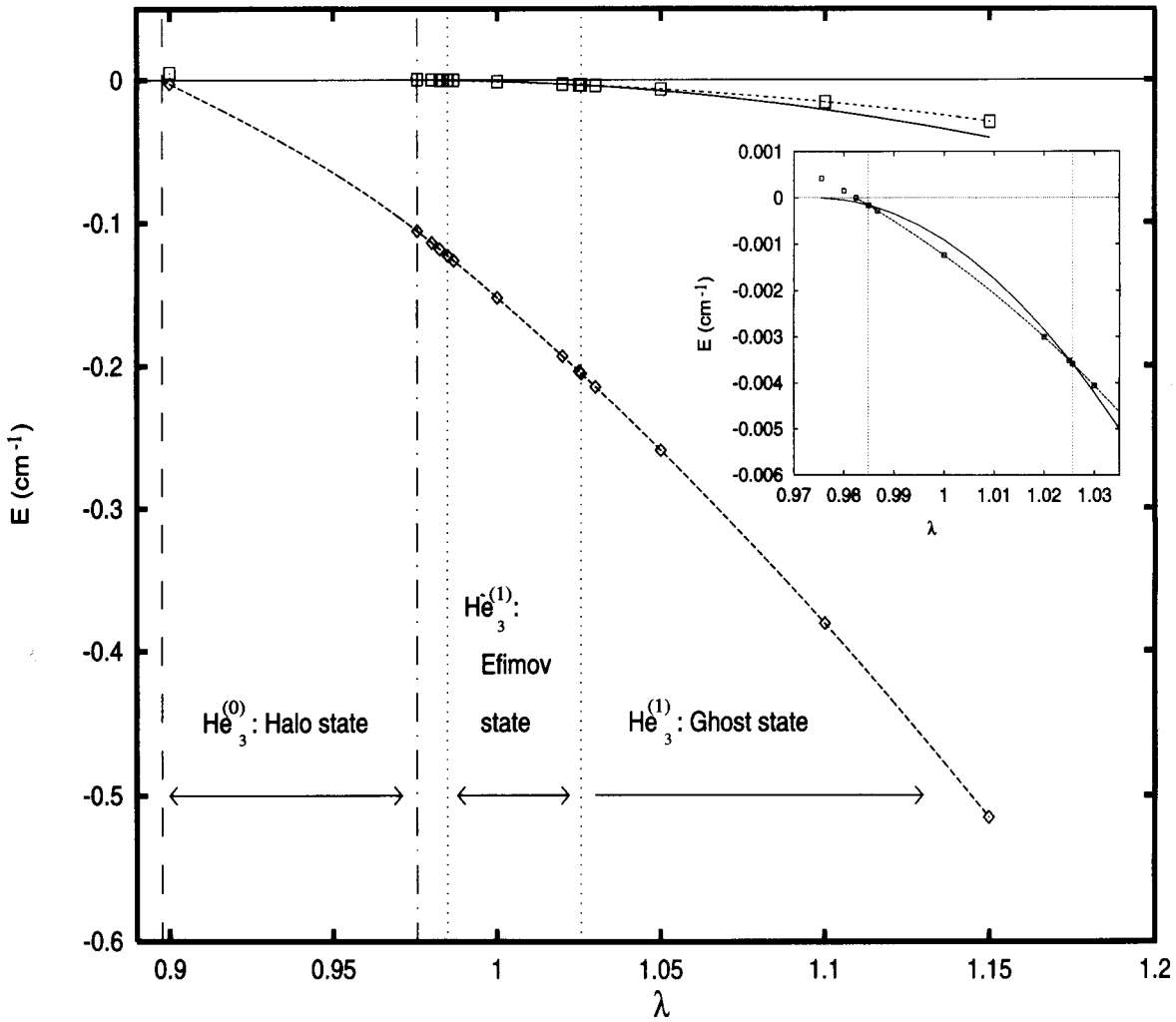

FIG. 4. Evolution of the bound states for the dimer and trimer (in cm^{-1}) as a function of the strength parameter, λ. The solid line corresponds to the dimer bound state and the dashed lines to the two trimer bound states. In each region of λ values (see text) the character of the bound states [He_3 ($k=0$), ground state and, He_3 ($k=1$), first excited state] is marked: halo, Efimov-type, and ghost state.

Figure 4 shows the values of the energies for the He_2 and He_3 ($k=0,1$) states when λ varies around one. In the inset of this figure an enhancement of the critical λ region is shown. Several regions in λ can be considered:

(i) between $\lambda_{halo}=0.8942$ and $\lambda_{2B}=0.9755$, where only a trimer bound state exists but not a dimer state; this type of trimer bound states are usually called halo states;

(ii) between $\lambda_{2B}=0.9755$ and $\lambda_{Efimov}=0.9849$, where the first excited state for the trimer begins to appear; this state could be characterized as a virtual state since it becomes bound state as the interaction increases;

(iii) between $\lambda_{Efimov}=0.9849$ and $\lambda_{ghost}=1.0256$, where the Efimov-type state is below the 2B continuum threshold and finally is overrun by this threshold; and

(iv) $\lambda>1.0256$ where the first excited state for the trimer is above the 2B continuum threshold and is generally called a ghost state.

The double crossing between the $E(He_3^{(1)})$ and $E(He_2)$ curves has been previously found.[7] Although the same potential[29] was employed in that case, the appearance of the excited state through the 2B continuum threshold was thought to occur for weakener values of the interaction, $\lambda_{Efimov}=0.9741$. Our λ_{Efimov} is close to the value found by Nakaichi-Maeda and Lim.[23] The limiting values of the λ parameter are slightly different from those suggested in Ref. 7 with a similar ratio $\lambda_{halo}/\lambda_{2B}=0.92$. In the literature of Nuclear Physics, this ratio is about 0.8. This discrepancy should be attributed to the long range nature of the molecular 2B interaction potential which behaves asymptotically differently from that of the nuclear interactions. It should be stressed at this point that in region (iii) only one Efimov-type state appears but no more. The striking result in our case is that this region includes $\lambda=1$, i.e., the case for which we consider the 2B interaction to be the correct physical interaction. This fact implies that the Efimov states must be quite elusive because very small fluctuations or uncertainties in the 2B interaction potential can lead to different conclusions about their existence. Furthermore, the different behavior with λ of the energies observed for the two states is explained as follows: from Fig. 3(a) it can be seen that the ground state is located in a region closer to the potential well

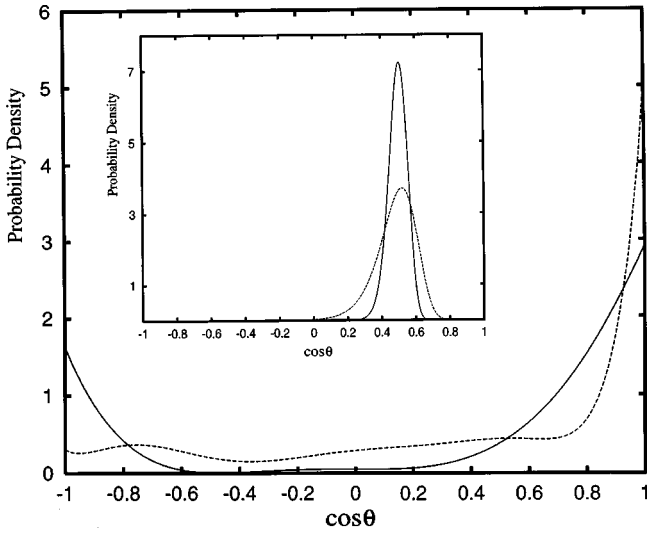

FIG. 5. Angular distributions for the ground $k=0$ (solid line) and first excited $k=1$ (dashed line) states of He_3. In the inset, the corresponding angular distributions for the ground states of Ar_3 (solid line) and Ne_3 (dashed line) are shown.

than the first excited state. This makes perfectly reasonable to find that tiny changes in the potential depth have a stronger effect on the ground level.

The analysis of the different triangular configurations (see Table IV) as described in Eq. (20) seems to reveal the clear predominance of scalene arrangements for both states (48.3% for the ground level and 74.3% for the excited level). However, for the ground state, the corresponding percentage comes from very small contributions of a high number of such basis functions. The second main configuration participating in the structure for this state is the quasilinear arrangement with 27.1%. Two more features allow us to conclude that the quasilinear arrangements play a decisive role in the geometry of the He_3 ground state. First, the level disappears if quasilinear ϕ_j functions are eliminated from the basis used in the calculation. And second, from the localization of the two maxima of $\mathcal{D}^{(0)}(R_1,R_2)$, its ratio being nearly equal to 2, we can deduce that they are strongly related to triangles with sides R_1, R_2 around 4.5 Å and R_3 being approximately equal to 8.8 Å. This preference for quasilinear disposition was also suggested through diffusion quantum MC calculations.[17] The need to include collinear arrangements in order to describe the floppy geometry of the ground state of He_3 may come from the fact that they can play the role of intermediate configurations among all of the possible triangular arrangements. Predictions concerning the geometrical shape of the excited state are not so clear since the contributions of isosceles configurations seem to be quite important. In any case, the equilateral configuration represents a negligible contribution.

The values of $\langle \cos\theta \rangle_0$ (see Table III) do not lead one to think of an equilateral configuration as the main arrangement for the ground level of the trimer. In this sense, our results are in total disagreement with some of the conclusions from previous MC calculations,[22,19] where the value for the bond angle was 60°. In Fig. 5, the angular distributions for both states ($k=0$ and $k=1$) are plotted. For comparison, in the inset of this figure, the angular distributions for the Ar_3 and Ne_3 clusters are also plotted but only for the ground state. These angular distributions have been calculated from the first seven momenta of $\cos\theta$. Whereas for Ar_3 and Ne_3 the cosine distribution is peaked near 0.5, indicating again an equilateral configuration a completely different behavior is observed for the ground state of He_3. We have two peaks (with a ratio of 1 to 2) for cosine values of -1 and $+1$, respectively, and a non-negligible probability of finding other types of angular arrangements. The distribution for the Efimov-type state is strongly peaked at $+1$ but again all the remaining angular arrangements are more or less equally probable, indicating the contribution of a great variety of triangular geometries, as confirmed by Table IV.

TABLE VII. Energies (in cm^{-1}), $E(X_n^{(k)})$, of the ground ($k=0$) and ($k=1$) excited states for the dimers ($n=2$) and trimers ($n=3$) of Ar (first column), Ne (second column) and He (third column). In the following rows, different combinations of the dimer levels are shown.

	Ar	Ne	He
$E(X_2^{(0)})$	−83.93	−16.56	−0.0009
$E(X_2^{(1)})$	−57.52	−1.88	
$E(X_3^{(0)})$	−252.43	−50.23	−0.1523
$E(X_3^{(1)})$	−220.91	−33.81	−0.0012
$3\times E(X_2^{(0)})$	−251.79	−49.68	−0.0027
$2\times E(X_2^{(0)})+E(X_2^{(1)})$	−225.38	−35.00	
$E(X_2^{(0)})+2\times E(X_2^{(1)})$	−198.97	−20.32	

An additional intrinsic difference among the clusters under study in this work is seen comparing the corresponding energies of trimers and dimers. Table VII shows these energy values for Ar (first column), Ne (second column), and He (last column). Energies for ground and first excited states of the dimers are shown in the first two rows. Notice the absence of an excited state for He_2. In the third and fourth rows, energies for the two first levels of the trimers are shown. Although they have already been listed in Table III, their inclusion here will facilitate comparison with the rest of entries of Table VII. The last three rows are for some combinations of ground and first excited state energies. In particular, the fifth row shows the value of three times the ground energy level of the dimers, while two times the dimer ground energy level plus the first excited energy level and vice-versa are shown in the sixth and seventh rows, respectively. Analysis of this table allows us to deduce the following relations for the ground levels of the different clusters:

$$E(\mathrm{Ar}_3^{(0)}) \sim 3\times E(\mathrm{Ar}_2^{(0)}),$$
$$E(\mathrm{Ne}_3^{(0)}) \sim 3\times E(\mathrm{Ne}_2^{(0)}), \tag{22}$$
$$E(\mathrm{He}_3^{(0)}) \ll 3\times E(\mathrm{He}_2^{(0)}),$$

and for the first excited states,

$$2\times E(\mathrm{Ar}_2^{(0)})+E(\mathrm{Ar}_2^{(1)}) < E(\mathrm{Ar}_3^{(1)}) < E(\mathrm{Ar}_2^{(0)})+2\times E(\mathrm{Ar}_2^{(1)})$$
$$2\times E(\mathrm{Ne}_2^{(0)})+E(\mathrm{Ne}_2^{(1)}) < E(\mathrm{Ne}_3^{(1)}) < E(\mathrm{Ne}_2^{(0)})+2\times E(\mathrm{Ne}_2^{(1)})$$
$$2\times E(\mathrm{He}_2^{(0)}) < E(\mathrm{He}_3^{(1)}) < E(\mathrm{He}_2^{(0)}), \tag{23}$$

whereas the energy for the ground level of Ar and Ne clusters is found to correspond approximately to three times the energy of the dimer ground level, such a description is not possible for the He system: $E(\mathrm{He}_3^{(0)})$ is about 50 times deeper than the value obtained considering the sum of three $E(\mathrm{He}_2^{(0)})$.

IV. CONCLUSIONS

As a result of the study carried out with this variational method in terms of pair coordinates, two bound states have been found for the He_3 cluster. The excited state presents an Efimov-type behavior in the sense that it is overrun by the 2B continuum threshold when the parameter λ multiplying the pairwise potential is varied and the associated bidimensional probability density function, $\mathcal{D}^{(1)}(R_1,R_2)$, presents large spatial extension. A non-negligible presence of the pair distribution function inside the potential well and the difficulties found to obtain unequivocally such an excited state (independent of the 2B potential and theoretical method used in the calculation) leads us to the conclusion that the possible Efimov state for the He_3 cluster is quite elusive and cannot as yet be definitely settled. Moreover, in the coordinates used here the kinetic energy operators of the total Hamiltonian, Eq. (7), do not present the clear behavior of an effective attractive long-range interaction of the $1/R^2$ type, with R being one of the given coordinates. We feel however that it should be instead the balance among all the terms involved in these kinetic operators which is responsible for the long-range interaction, at least for distances larger than r_0, the effective range of the 2B potential.

The quantitative analysis of the different geometrical configurations contributing to each triatomic bound state leads us to the following conclusion about the He_3 system: the ground state is found to be formed by a considerable component of quasilinear arrangements, whereas contributions from a large number of different triangular configurations seem to be necessary in order to explain the geometry of the first excited state. Those quasilinear arrangements are thought to play the role of intermediate configurations in the transit to other triangular arrangements in the case of the ground state. The importance of equilateral configurations increases when the Ne_3 and specially Ar_3 systems are considered. A marked difference concerning the rigidity of the trimers is found when the He_3 system is compared with the two other systems in this work: while dispersions or fluctuations extracted from the helium trimer about its spatial extension (average triangle side and area) have high values, the results for the Ar_3 and Ne_3 allow us to conclude the presence of more compact and rigid structures for these systems. In this sense we find a clear connection between the equilateral condition and rigidity, whereas the importance of quasilinear arrangements in the geometry of the ground state of the He_3 system seems to be related to its extremely floppiness. We would also like to point out that by using this kind of coordinates one can estimate the weight of the different geometrical configurations and therefore it is possible to know their contributions to each bound state. As far as we know, this is the first ''exact'' variational calculation including the proper symmetry of the problem.

The final point is to suggest from our results some possible ways of detecting Efimov-type states. Recently, He dimers and trimers have been detected by diffraction from a transmission grating leading to a nondestructive mass selection.[12] The signal corresponding to He trimers has not been resolved in terms of different bound states of the system. The diffraction grating was built with a period of 200 nm with bars and slits of equal size. According to our estimates, trimers can pass through this kind of gratings independently of the bound states which are populated in the experiment. The question now is to envisage a way to select or discriminate one of these two bound states. The average diameter of the circumscribed circumferences for all of the triangular configurations is 10.87 ± 3.55 Å for the ground state and 69.11 ± 25.95 Å for the excited state (for the quasilinear configurations, such a diameter is chosen to be equal to the largest side). Due to this difference, if the grating is tilted at different incident angles from the He beam, the effective slit can be of the order of the average diameter of the Efimov-type state and therefore it would be possible to filter such a state. From the different population (and if the experimental resolution in intensity is good enough) it could be possible to detect it in an indirect way. Alternatively, such states could also be indirectly measured or observed from the kinetics of formation of the dimers and trimers in He beams,[43] three-body recombination of ultracold atoms[44] and from the properties of liquid helium. In this last case, a complete different dynamics could be developed considering that the He dimer interaction potential is affected by the surroundings in many ways similar to those which we have simulated by varying the λ value and therefore dimers and trimers could play a very important role when one analyzes the well known properties of He liquid.

ACKNOWLEDGMENTS

This work has been supported in part by DGICYT (Spain) under Contract No. PB95-0071, Spanish-Cuban Project between CSIC and Agencia de Ciencia y Tecnologia Cubana, and the Research Network with Contract No. FMRX-CT96-0088. We would like to thank to W. Schöllkopf, M. Lewerenz, and J. P. Toennies for many interesting and fruitful discussions.

[1] V. Efimov, Phys. Lett. **33B**, 563 (1970); Nucl. Phys. **A210**, 157 (1973); Sov. J. Nucl. Phys. **12**, 589 (1971).
[2] R. G. Newton, *Scattering Theory of Waves and Particles*, 2nd ed. (Springer, Berlin, 1982).
[3] R. D. Amado and J. B. Noble, Phys. Lett. **35B**, 25 (1971).
[4] A. C. Fonseca, E. F. Redish, and P. E. Shanley, Nucl. Phys. **A320**, 273 (1979).
[5] T. K. Lim, S. K. Duffy, and W. C. Damert, Phys. Rev. Lett. **38**, 341 (1977).
[6] Th. Cornelius and W. Glöckle, J. Chem. Phys. **85**, 3906 (1986).
[7] B. D. Esry, C. D. Lin, and C. H. Greene, Phys. Rev. A **54**, 394 (1996).
[8] T. González-Lezana, J. Rubayo-Soneira, S. Miret-Artés, F. A. Gianturco, G. Delgado-Barrio, and P. Villarreal, Phys. Rev. Lett. **82**, 1648 (1999).
[9] F. Luo, G. C. McBane, G. Kim, C. F. Giese, and W. R. Gentry, J. Chem. Phys. **98**, 3564 (1993).
[10] F. Luo, G. C. McBane, G. Kim, C. F. Giese, and W. R. Gentry, J. Chem. Phys. **100**, 4023 (1994).

[11] E. S. Meyer, J. C. Mester, and I. F. Silvera, J. Chem. Phys. **100**, 4021 (1994).
[12] W. Schöllkopf and J. P. Toennies, Science **266**, 1345 (1994); J. Chem. Phys. **104**, 1155 (1996).
[13] H. S. Huber and T. K. Lim, J. Chem. Phys. **68**, 1006 (1978).
[14] Y.-H. Uang and W. C. Stwalley, J. Chem. Phys. **76**, 5069 (1982).
[15] A. K. Motovilov, S. A. Sofianos, and E. A. Kolganova, Chem. Phys. Lett. **275**, 168 (1997).
[16] S. Huber, Phys. Rev. A **31**, 3981 (1985).
[17] M. Lewerenz, J. Chem. Phys. **106**, 4596 (1997).
[18] R. N. Barnett and K. B. Whaley, Phys. Rev. A **47**, 4082 (1993).
[19] M. V. Raman Krishna and K. B. Whaley, J. Chem. Phys. **93**, 6738 (1990).
[20] R. A. Aziz, V. P. S. Nain, J. S. Carley, W. L. Taylor, and G. T. McConville, J. Chem. Phys. **70**, 4330 (1979).
[21] D. M. Leitner, J. D. Doll, and R. M. Whitnell, J. Chem. Phys. **94**, 6644 (1991).
[22] S. W. Rick, D. L. Lynch, and J. D. Doll, J. Chem. Phys. **95**, 3506 (1991).
[23] S. Nakaichi-Maeda and T. K. Lim, Phys. Rev. A **28**, 692 (1983).
[24] T. R. Horn, R. B. Gerber, J. J. Valentini, and M. A. Ratner, J. Chem. Phys. **94**, 6728 (1991).
[25] D. M. Leitner, R. S. Berry, and R. M. Whitnell, J. Chem. Phys. **91**, 3470 (1989).
[26] E. Nielsen, D. V. Fedorov, and A. S. Jensen, J. Phys. B **31**, 4085 (1998).
[27] V. Spirko, P. Jensen, P. R. Bunker, and A. Čejchan, J. Mol. Spectrosc. **112**, 183 (1985); J. K. G. Watson, Can. J. Phys. **72**, 238 (1994); Chem. Phys. **190**, 291 (1995).
[28] I. P. Hamilton and J. C. Light, J. Chem. Phys. **84**, 306 (1986).
[29] R. A. Aziz and M. J. Slaman, J. Chem. Phys. **94**, 8047 (1991).
[30] R. A. Aziz and M. J. Slaman, Chem. Phys. **130**, 187 (1989).
[31] R. A. Aziz and M. J. Slaman, Mol. Phys. **58**, 679 (1986).
[32] A. García-Vela, P. Villarreal, and G. Delgado-Barrio, J. Chem. Phys. **94**, 7868 (1991); A. García-Vela, R. B. Gerber and U. Buck, J. Phys. Chem. **98**, 3518 (1994).
[33] A. Bhattacharya and J. B. Anderson, J. Chem. Phys. **100**, 8999 (1994); C. A. Parish and C. E. Dykstra, *ibid.* **98**, 437 (1993).
[34] A. R. Janzen and R. A. Aziz, J. Chem. Phys. **103**, 9626 (1995).
[35] P. O. Löwdin, Adv. Phys. **5**, 1 (1956).
[36] L. W. Bruch and I. J. McGee, J. Chem. Phys. **52**, 5884 (1970).
[37] A. J. Thakkar and V. H. Smith, Mol. Phys. **27**, 593 (1974).
[38] D. E. Beck, Mol. Phys. **14**, 311 (1968); **15**, 332 (1968).
[39] Y. C. Tang and R. C. Herndon, Physica (Utrecht) **31**, 1143 (1965); J. De Boer and A. Michels, *ibid.* **5**, 332 (1938).
[40] L. J. Burgmans, J. M. Farrar, and Y. T. Lee, J. Chem. Phys. **64**, 1345 (1976).
[41] R. A. Aziz, F. R. W. McCourt, and C. C. K. Wong, Mol. Phys. **61**, 1487 (1987).
[42] K. T. Tang, J. P. Toennies, and C. L. Yiu, Phys. Rev. Lett. **74**, 1546 (1995).
[43] L. W. Bruch, S. Miret-Artés, W. Schöllkopf, and J. P. Toennies (unpublished).
[44] P. O. Fedichev, M. W. Reynolds, and G. V. Shlyapnikov, Phys. Rev. Lett. **77**, 2921 (1996).